submitted: 09.12.2024. *Scientific research paper*
corrected: 31.01.2025. *UDC 620.193:624.21*
accepted: 01.02.2025. *https://doi.org/10.62683/ZRGAF40.1*

PROBABILISTIC ESTIMATION OF LIFE-CYCLE CHLORIDE-INDUCED CORROSION

Jiabin Liu[1]
Heng Mei[2]
Andrija Zorić[3]

Abstract

Coastal bridges constitute critical components for the transportation in offshore areas, and thus their serviceability and safety against hazard such as earthquakes need to be ensured in a life-cycle perspective. However, coastal bridges are confronted with significant corrosion that results in degradation effects mainly on concrete piers. This can make the resistance property of bridge diverse from the initially designed state. Hence, it is vital to predict the residual performance of coastal bridges throughout its life-cycle period. Prior studies described the corrosion evolvement using mostly deterministic methods, whereas the uncertainty was neglected in terms of both the corrosion environment and concrete performance. In this study, the corrosion developed of bridge pier was investigated probabilistically. A convolutional formula was proposed to account for the correlation between the initial corrosion time and the remained time to the expected lifetime. The proposed approach was validated using a prototype bridge in China, where the corrosion environment was captured by historical chloride data, the uncertainty in other parameters was reflected using random variables. The results showed that the proposed method can well apply to predicting the corrosion state in the bridge life-cycle period, where the initial corrosion time approaches closely to skewed distribution. The selected bridge exhibited notable corrosion likelihood at the end of lifetime. It was found that the probability of corrosion absence is approximately 30% while the maximum loss mass ratio reaches around 45% for the lifespan of 100 yrs. The proposed method can be further used to determine the degraded performance for bridge analysis under other impacts such as earthquakes and waves.

Key words: *Chloride-induced corrosion; Coastal bridge; Life-cycle; Probabilistic.*

[1] PhD, Associate professor, Harbin Institute of Technology, China, liujiabin@hit.edu.cn, ORCID 0000-0001-8304-9712
[2] PhD candidate, Harbin Institute of Technology, China, 19B933031@stu.hit.edu.cn, ORCID 0009-0001-4884-5315
[3] PhD, Assistant Professor, University of Niš, Serbia, andrija.zoric@gaf.ni.ac.rs, ORCID 0000-0002-3107-9204

1. INTRODUCTION

Coastal bridges were built to connect the districts separated by bays, leading to their great importance in the transportation of community and resources. Whereas, these structures were threatened by a number of unfavorable effects, among which earthquakes can bring about direct load impact while the corrosion action can give rise to the declined capacity. Chloride-ion is the main cause of corrosion in oceanic environment. The combined effects of both events pose significant threats to coastal bridges, and the risk develops as the service time expands [1]. Hence, it is vital to predict the corrosion state so as to supply guidance for repairing and retrofitting.

The corrosion process consists of two phases including the initiation of corrosion and the development of corrosion effects [2]. For the reinforcement-concrete (RC) bridge, the corrosion initiation depends on the chloride-ion that penetrates concrete cover and erodes the strengthened reinforcement [3]. Many studies have been conducted to predict this parameter given environmental conditions.

Tuutti [4] suggested to describe the process of ion penetration using the second Fick's law. Kassir [5] studied the influence of chloride-induced corrosion on the reinforced-concrete bridge decks, in which a closed-form formula was proposed to predict the corrosion initiation time using the ion accumulation data from measurements. Their results showed that the constant concentration can cause underestimation towards the imitation time. Lin [6] proposed a dynamic corrosion rate model based on Bulter–Volmer kinetics, with a rust expansion model also developed based on Faraday's law. A comparison between their model and experimental results validated the accuracy and reliability of the mathematical method. Khan [7] conducted a review research upon the estimation method of the initial corrosion time. Reviewing prior researches shows that, the initiation time is affected by multiple factors that are all highly uncertain within the life-cycle period of bridges. Therefore, using the probabilistic method to describe such process is more suitable comparing to the deterministic method.

Precedent studies have implied that corrosion can affect the bridge performance mainly by undermining the rebar resistance [8], while some have also addressed their influence on the concrete material and the bonding effects between concrete and rebar [9]. In this study, the corrosion effect was reflected with emphasis on the rebar component. Enright [10] studied the degraded resistance of reinforced concrete bridge beam subjected to chloride-induced corrosion. The flexure strength loss in a concrete bridge was addressed in their study, with various factors considered to compare the effects on the remain effective steel area and beam performance. Ghosh [11] investigated the time-varying fragility of a bridge under the joint effects of earthquake and corrosion-induced degradation. The formulation was developed to consider the time-dependent feature, with the distinct degradation rate in various bridge components also considered to reflect the realistic situations. Dizaj [12] inspected the vulnerability of corroded RC frames within their service life. The pitting corrosion effects were highlighted in their research, showing that the variability of pitting corrosion has insignificant influences on the global failure of bridge. Liu [13] conducted an experimental research to examine the remained materials after major corrosion effects, showing that phases of steel rust in the atmospheric zone were lepidocrocite and goethite, while lepidocrocite and maghemite dominate in the tidal zone. Tian [14] conducted research to analyze the steel corrosion using historical data obtained from natural environments. Their research focused on the corrosion rate, microstructure at the steel-concrete interface, rust composition and properties. And the analysis indicated that the natural corrosion rate of steel tends to decrease over time in long terms. It is then evident that the eroded materials can undermine the rebar performance in terms of both the section area and strength property.

The coastal bridges in seismic-prone areas, such as the west coast of USA, and Japan, are also exposed to the high seismic risk. Historical post-hazard survey has shown that bridges piers were significantly damaged or even collapsed during strong ground motions [15][16]. And this can be further escalated by the joint actions of both hazards due to the declined capacity.

The literature review shows that the corrosion influence was characterized from deterministically to probabilistically by accounting for the uncertainty in the chloride-ion environment. However, existing research often adopted a simulation method to obtain the corrosion uncertainty after certain service time, in which the initiation time and the corrosion state were sampled according to the corrosion environment. Such method requires to run the sampling operation for each corrosion period, leading to poor efficiency for a life-cycle investigation. To this end, the probabilistic estimation of corrosion was highlighted in this study. An analytical method was presented to anticipate the corrosion degree at arbitrary time, so as to improve the efficiency for other analysis. A case study was performed to validate the proposed method, where the historical data was employed to capture the chloride uncertainty. The analysis results showed good applicability of the proposed method in predicting the corrosion as per the service time. It was found that there exists both upper and lower bounds for the corrosion state, and they were prone to rise with increasing rate as the service time becomes longer.

The primary contents of this study were structured as follows: 1) the analytical model for corrosion prediction was developed in Section 2, where the initiation time and corrosion influence were illustrated; 2) a case study was demonstrated in the third section, where the prototype bridge and the site-specific data were employed. Besides, a reliability analysis was conducted to obtain the failure probability of the bridge subjected to the design acceleration; 3) the conclusion remarks were drawn in the final section.

2. PROBABILISTIC LIFE-CYCLE CORROSION ESTIMATION

2.1. Initiation corrosion time and corrosion effects

Estimating the initiation corrosion time is crucial because it determines the time left for the corrosion development. The initiation time is affected by multiple factors including the ion concentration, cover depth, critical concentration for the corrosion onset, and concrete properties. On this basis, the erosion process starts when the ion concentration at the cover depth reaches the critical value, as shown in **Fig. 1**. And the initiation time can be estimated by the following equation when the primitive chloride concentration is negligible [17],

$$T_{init} = \left\{ \frac{d_c^{\ 2}}{4k_e k_t k_c D_0 \left(t_0\right)^n} \left[erf^{-1} \left(\frac{C_s - C_{cr}}{C_s} \right) \right]^{-2} \right\}^{1/(1-n)} \quad (1)$$

in which d_c is cover depth, D_0 is the diffusion rate of ion penetration, and t_0 is the curing time of concrete material. k_e , k_t , k_c are factors employed to reflect concrete properties, which corresponds to the influences of environment, temperature and the curing condition. C_s and C_{cr} are the ion concentration near the bridge pier and the critical value, respectively. Besides, n is the age factor that reflects the declined corrosion rate with time.

Reviewing existing research showed that the chloride-induced corrosion primarily results in the loss of section area and strength for steel reinforcements. The influence on concrete is also associated with the strength decline in the rebar as it further leads to the lowered confinement to concrete [18]. In this study, the rebar corrosion was highlighted because of its dominant influences on the flexure behavior of bridge piers [10].

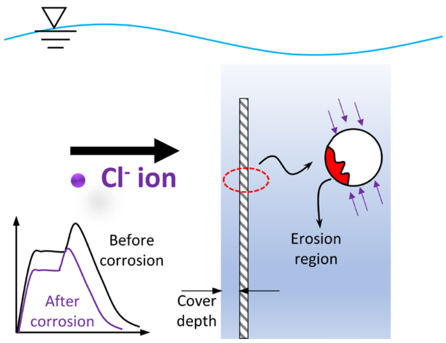

Figure 1. Diagram of corrosion initiation and progression

Many researches have implied the correlation between corrosion rates and the current density due to the corrosion process. And the time-varying diameter of rebar can be expressed in the following form [11]:

$$d_s\left(t\right) = \begin{cases} d_{s0}, t \le T_{init} \\ d_{s0} - 2\int_{T_{init}}^{t} \lambda\left(t\right) dt, T_{init} < t \le T_f \\ 0, t > T_f \end{cases} \quad (2)$$

Note that d_{s0} is initial rebar diameter, t is the time since the corrosion onset, and T_f refers to the time when the rebar is completely eroded. In addition, $\lambda\left(t\right)$ is the corrosion rate affected by the current density, which takes the form as follows:

$$\begin{cases} i_{corr}\left(t\right) = 0.85 i_{corr,0} \left(t - T_{init}\right)^{-0.29}, t \ge T_{init} \\ i_{corr,0} = \dfrac{37.5\left(1 - w/c\right)^{-1.64}}{d_c} \mu A / cm^2 \end{cases} \quad (3)$$

in which $i_{corr,0}$ is the current density at the initial stage, w/c is cement-water ratio, while other parameters are defined in alignment with Eq. (1). Accordingly, the mass reduction ratio (Q_{corr}) can be calculated using the below formula:

$$Q_{corr}(t) = 1 - \left(d_s(t)/d_{s0}\right)^2 \tag{4}$$

Prior research suggested that corrosion can also give rise to the reduced strength of steel rebar, and the reduction was correlated to the mass loss via the equation as follows:

$$f_y = \left(1 - \alpha_y Q_{corr}\right) f_{y0} \tag{5}$$

in which f_{y0} is the yielding strength at the initial stage, while α_y is the decrease rate of rebar strength. And it is taken as 4.9×10^{-3} in the current research.

2.2. Proposal of lifetime corrosion model

To improve the efficiency of corrosion analysis throughout the life-cycle period of bridges, an approximate lifetime corrosion model was proposed in the current work. To begin with, the uncertainty in the initiation time can be characterized by a random distribution $f_{T_{init}}(t)$ by fitting the data from Monte Carlo modeling in accordance to **Eq. (1).** Besides, the corrosion degree can be also determined for the residual time depending on the designed lifetime or the inspected operation time. Consequently, the erosion progress can be characterised by the following equation in according to the whole probability theory:

$$P_{CR}\left(CR{=}cr_i\right){=}\sum P_{CR}\left[CR = cr_i \middle| T = T_i, T_L = t_l\right]\cdot P\left(T = T_i\right) \tag{6}$$

where $P(T = T_i)$ represents the likelihood that the corrosion starts at T_i, and P_{CR} is the probability of corrosion state $CR = cr_i$ conditional on a design lifetime of T_L. Such equation can be further modified into the following form when the initiation time is continuous as:

$$\begin{cases} f_{CR}(cr) = \int_0^{T_L} f_{CR}\left(cr \middle| T_R\right)\cdot f_T(t)\,dt \\ F_{CR}(cr) = \int_0^{T_L} F_{CR}\left(cr \middle| T_R\right)\cdot f_T(t)\,dt + \int_{T_L}^{+\infty} f_T(t)\,dt \end{cases} \tag{7}$$

in which f_{CR} is the probability density function of corrosion state given the residual corrosion time $T_R = T_L - t$, and f_T signifies the probability density of the initiation time and is equal to $f_{T_{init}}(t)$ derived from regression analysis. In addition, the last term of integral from TL to infinite is used to reflect the absence of corrosion within the bridge lifespan. The above equation accounts for overall possible initiation time throughout the life time T_L in the upper integral limit, as illustrated in Fig. 2.

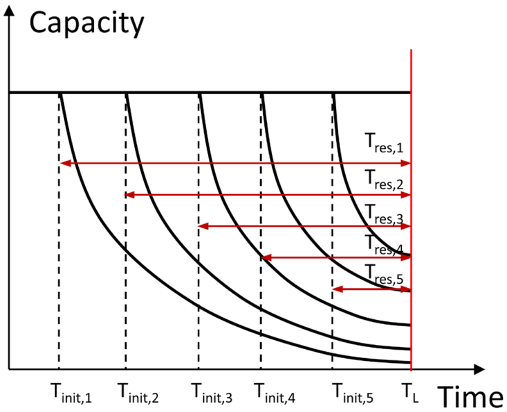

Figure 2. Relationship of initiation and residual time in lifetime model.

On this basis, the probability function of corrosion state can be deducted by only calculating the corrosion development in the specified residual time by separating the design life time into multiple intervals. And the corrosion at other residual time can be approximately obtained by correlating the density function with time-dependent factors as follows:

$$\begin{cases} f_{CR}\left(cr \mid T_R\right) = f_{CR}\left(cr \mid T_R\left(t\right); \alpha_1\left(T_L - t\right), \alpha_2\left(T_L - t\right), \cdots, \alpha_n\left(T_L - t\right)\right) \\ F_{CR}\left(cr \mid T_R\right) = F_{CR}\left(cr \mid T_R\left(t\right); \alpha_1\left(T_L - t\right), \alpha_2\left(T_L - t\right), \cdots, \alpha_n\left(T_L - t\right)\right) \end{cases} \tag{8}$$

where $\alpha_1\left(T_L - t\right) \sim \alpha_n\left(T_L - t\right)$ are the corrosion density function within the residual corrosion time $\left(T_L - t\right)$. Furthermore, the uncertain corrosion distribution at arbitrary time of the bridge lifetime can be computed using the integral formula in **Eq. (7)**.

3. CASE STUDY

3.1. Information of prototype bridge

To validate the effectiveness of the proposed method above, a case study was carried out to demonstrate the corrosion analysis. Besides, a reliability analysis was also conducted to inspect the time-varying security of degraded bridges. A prototype bridge in China coastal area was chosen for this purpose, whose designed lifespan is 100 yrs. **Fig. 3** shows the geometry setups of the selected bridge, which consists of two spans with equal length at 30 m. The girder employs a box-shape section, with length and height equal to 12 m and 2.6 m, respectively.

More detailed configuration of the girder component can be found in this figure. The bridge pier is designed as single column with circular section, where the diameter is set to 1.6 m. The reinforcement configuration inside the pier section (40Φ25), and the pier height is set identically at 10.5 m for each span. The bridge girder is supported by the bent-cap (2.5 m height and 1.9 m width) casted on the pier top. The girder component was connected to the bent using high-strength bearings alongside adequate constrainers to ensure the force delivered between super- and sub-structures. As a result, the shear and flexure failure modes at the pier bottom dominate in contrast to the possible joint flexure failure for a rigid-frame bridge. All the bridge components are constructed using C35 concrete and HRB400 rebar, where the compressive and yielding strengths are 35 MPa and 400 MPa, respectively. Further, the cover depth of bridge piers is expanded to 80 mm to resist against the high-diffusion environment.

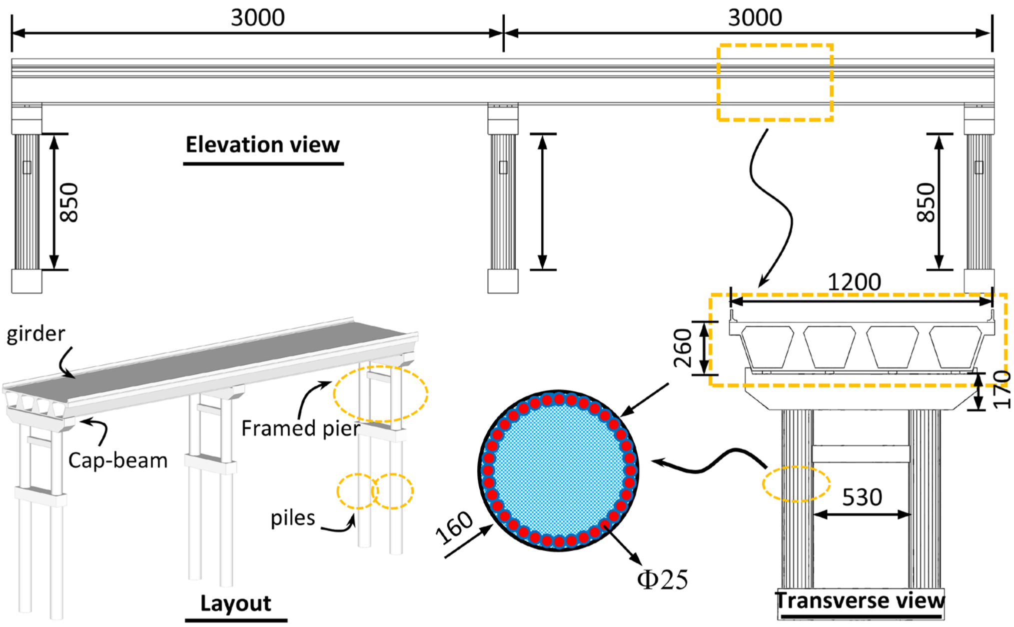

Figure 3. Configuration of prototype bridge (unit = cm).

3.2. Corrosion analysis

The chloride-ion environment is required to perform corrosion analysis according to **Eq. (1)**. To this regard, the concentration in sea water was collected from the Chinese Ocean Science Data (COSC) platform, and the observation data from 1986 to 2016 (30 yrs) was adopted for our analysis. **Fig.4** indicates the monthly variation of the ion concentration. It can be found that the concentration value reaches the maximum in November, and continue to remain high in adjacent months including December and January. In contrast, the ion concentration turns lower at the middle of the year, from June to August.

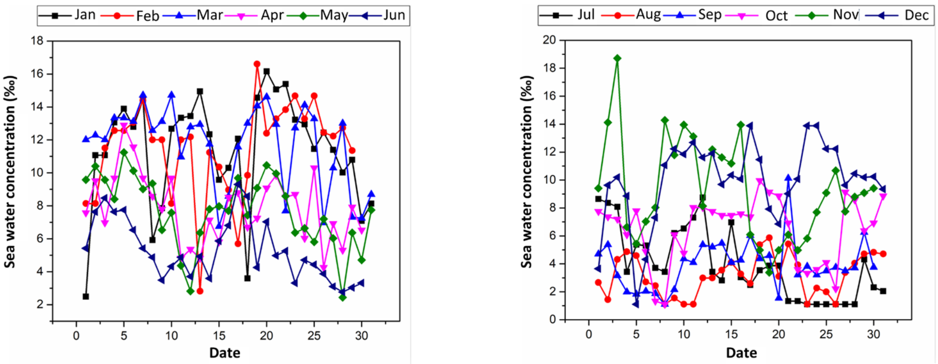

Figure 4. Monthly ion concentration in sea water near selected bridge (1996): (a) Jan. – Jun.; (b) Jul. – Nov.

Using the historical concentration data, the statistic analysis was demonstrated to describe the uncertainty in chloride-ion condition. **Fig. 5(a)** presents the histogram of ion concentration, along with the empirical cumulative probability (ECDF). On this basis, the ion concentration was hypothesized to approach normal distribution, and the distribution parameter can be attained using the regression analysis, as indicated in **Fig. 5(b)**. Moreover, the concentration of chloride-ion can be calculated using a ratio relationship, see **Eq. (9)**. Note that $S\,\%_{00}$ and $Cl\,\%_{00}$ are the concentration of overall ion and chloride only, respectively. This leads to the normal distribution of chloride ion with $\mu = 4.23$ and $\sigma = 2.22$.

$$S\,\%_{00} = 1.80655\,Cl\,\%_{00} \tag{9}$$

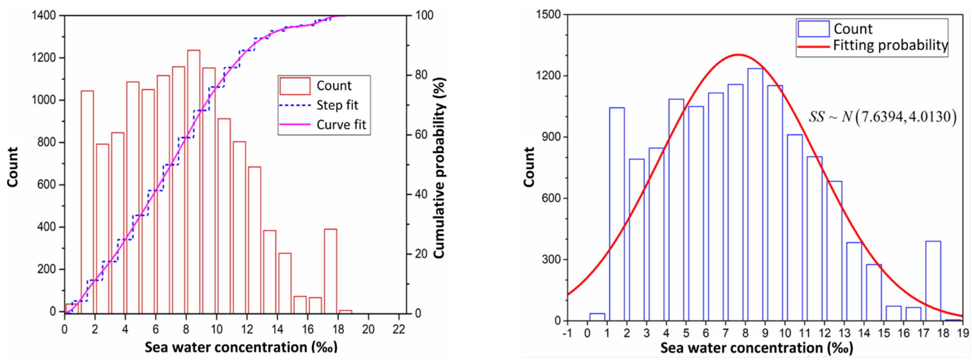

Figure 5. Statistical analysis on ion concentration near selected bridge: (a) histogram and ECDF; (b) normal distribution fitting.

Prior research has shown that the cement-water ratio can substantially influence the diffusion rate (D_0) [19]. On this basis, this parameter was calculated for the high-strength concrete (≥50 MPa), see **Eq. (10)**.

$$D_0 = 2.519\frac{m_W}{m_{(C+B)}} - 0.681\frac{m_{FA}}{m_{(C+B)}} - 0.04816 \tag{10}$$

in which m_W is the water mass, $m_{(C+B)}$ is the overall mass of cement and grains, while m_{FA} is the mass of fly ash powder as additives. The concrete component consists of cement (202 kg), water (167 kg), fly ash powder (314 kg), grains (1709 kg) for unit stere. And this leads to the initial diffusion rate at 15.67 mm/ yr. In addition, the factors (k_e, k_t, k_c) in **Eq. (1)** were also designated with uncertainty using normal distribution. The mean value was set to 0.79 and 2.70 for k_e and k_t, while the curing factor takes 1.0 for a standard curing treatment. The coefficient of variance (Cov) was specified at 1.48 for k_e and k_t, while 1.05 was assigned to the curing factor.

Additionally, the threshold ion concentration for the corrosion process to begin is determined in accordance to the Duracrete report, and the value at distinct position along the pier height was presented in **Table 1**. The threshold value depends on the cement-water ratio, leading to the distribution of $N(0.89, 0.15)$ using interpolation. Note that only the tidal-splash zone was considered here because the prototype bridge uses a high-rise pile cap. Based on this, the corrosion analysis can be carried out in accordance to Section 2.

Table 1. Threshold chloride concentration at corrosion onset [19]

Corrosion environment	Cement-water ratio (w/c)	Distribution of critical chloride concentration
Underwater	0.3	*N*(2.3,0.2)
	0.4	*N*(2.1,0.2)
	0.5	*N*(1.6,0.2)
Tidal-splash zone	0.3	*N*(0.90,0.15)
	0.4	*N*(0.90,0.13)
	0.5	*N*(0.50,0.10)

4. DISCUSSION ON RESULTS

Fig. 6 indicates the initiation corrosion time when the concentration at the cover depth equals the threshold value. It can be seen that the highest probability density occurs at around 12 yrs, while the median value of initiation time was obtained at 23 yrs. In addition, the probability of corrosion occurrence within the bridge lifespan was approximately 72%, compared to only 3% during the first 10 yrs. Building upon this basis, the regression analysis was performed by fitting the data. To this regard, an logarithmic Gumbel distribution (**Eq. (11)**) was introduced herein to align with the modeling results, and the comparison of modeling and analytical ECDF curves were also compared in **Fig. 6**. It is clear that the regressed distribution matches well with the sampling outcome, showing good applicability of the proposed method.

$$F_T(t) = \exp\left[-\exp\left(-\frac{\ln t - 3.333}{1.232}\right)\right], t > 0 \tag{11}$$

$$f_T(t) = \exp\left[-\exp\left(-\frac{\ln t - 3.333}{1.232}\right)\right] \cdot \left[-\exp\left(-\frac{\ln t - 3.333}{1.232}\right)\right] \cdot \left(-\frac{1}{1.232}\right) \cdot \frac{1}{t} \tag{12}$$

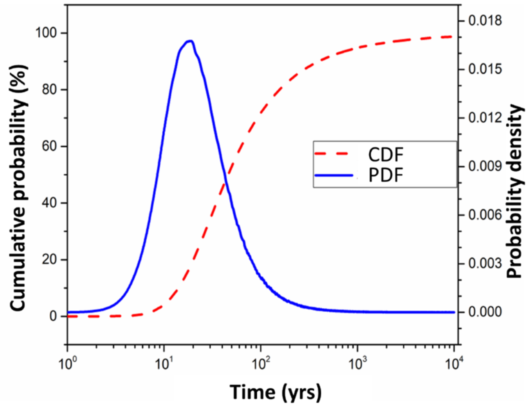

Figure 6. Modeling results of initiation corrosion time.

Additionally, the corrosion development during the residual life time was analyzed using **Eqs. (2)-(5)**, leading to the distribution of mass reduction ratio in **Fig. 7(a)**. It can be found that the erosion-induced mass loss rises significantly as the residual time increases. The median value increases from 8% (10 yrs) to 40.5% (100 yrs). The mass reduction corresponding to the median initiation corrosion time (23 yrs) is 32.8%, showing that nearly 1/3 steel material was eroded during the following 77 yrs. The maximum value of the reduction ratio remains lower than 60% across overall residual corrosion time. This implies the minimal likelihood for the rebar to be completely eroded. On this basis, the fitting analysis was also applied in accordance to **Eq. (8)**. And the Gumbel distribution (**Eq. (13)**) was employed here to fit the data in **Fig. 7(a)**, with the results shown in **Fig. 7(b)**.

$$F_{CR}\left(cr;\mu(t),\beta(t)\right)=\exp\left[-\exp\left(-\frac{x-\mu(t)}{\beta(t)}\right)\right] \tag{13}$$

in which $\mu(t)$ and $\beta(t)$ are both the parameters in Gumbel distribution, and they are correlated to the time variable (t) to reflect the corrosion development with time. The power function was utilized here for the fitting analysis. As can be seen in **Fig. 7(b)**, the fitting curve shows good agreement with the parameter from the regression analysis. Hence, the corrosion state at arbitrary time of the bridge lifespan can be computed via **Eq. (8)**.

Fig. 8 displays the distribution of mass reduction ratio at various service periods, including 20, 50, 70 and 100 yrs. Accordingly, the diameter reduction ratio and the strength reduction ratio were also included. It can be seen here that, the probability density remains comparable within certain ranges for different period examined. For example, the result at T = 50 yrs coincides with T = 25 when the mass ratio (Q_{corr}) is lower than 0.1. Also, T = 75 yrs yields similar results as T = 50 yrs before Q_{corr} rises to 0.23. The probability density of diameter reduction exhibits comparable results, see **Fig. 8(b)**. By contrast, the maximum value of strength reduction takes merely 0.2 owing to the multiplication factor in **Eq. (5)**.

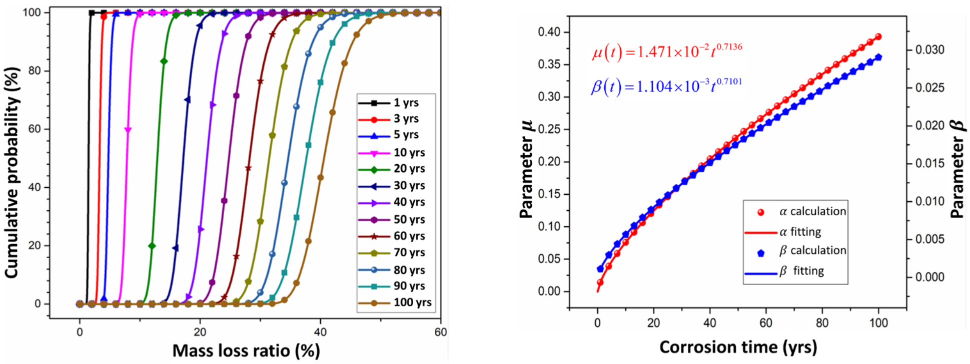

Figure 7. Modeling results of corrosion in residual life time: (a) mass reduction ratio; (b) parameter regression.

The cumulative probability was shown in the (b) subplot. It can be found that the corrosion probability increases as the considered time period becomes longer. The initial values at Q_{corr} = 0 increases from 0.3 to over 0.7 for the period equal to 20 and 100 yrs, respectively, as shown in **Fig. 8(a)**. This shows the essential influences of corrosion on the bridge with long lifespans. The initial value here is larger than zero because of the last term in **Eq. (7)**, which implies the initial corrosion time exceeds the designed lifespan of bridges. Therefore, the above proposed method can well predict the corrosion evolution without repeated sampling demand.

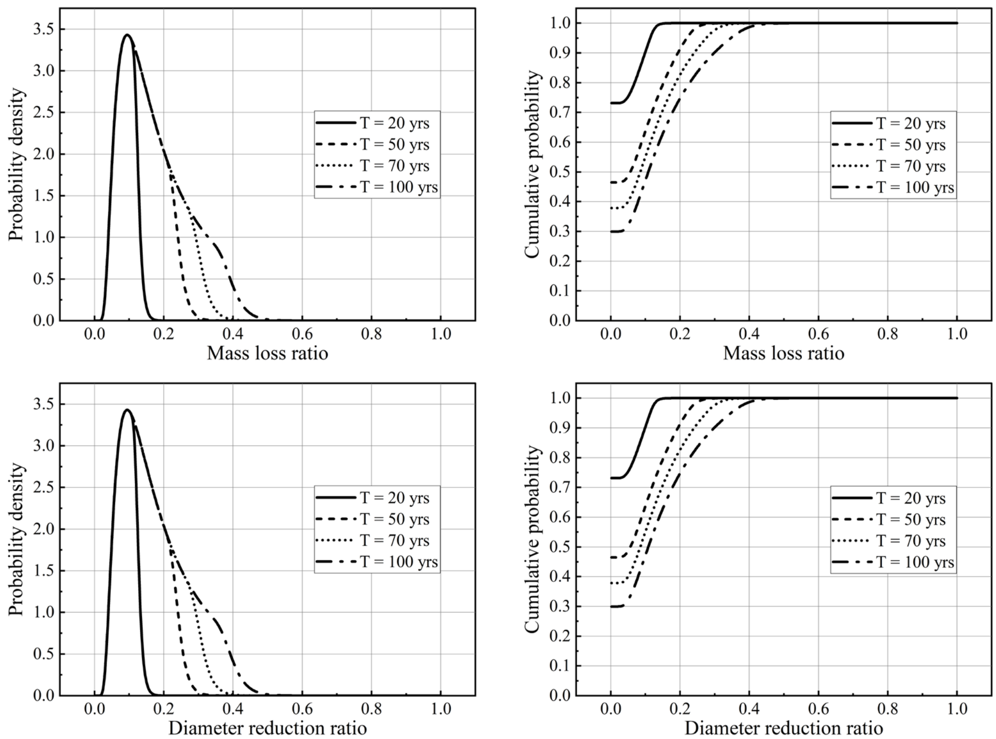

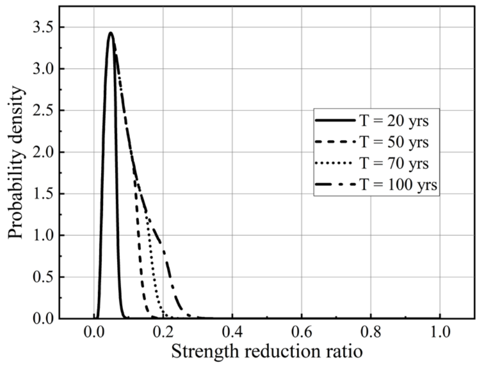

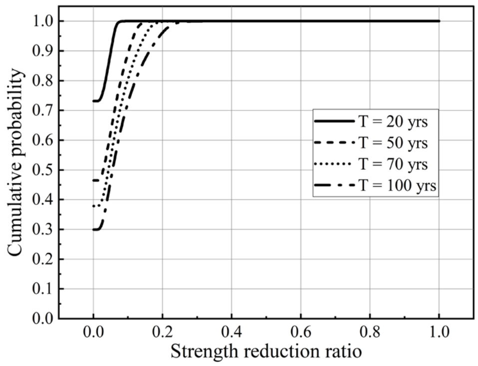

Figure 8. Estimated corrosion effects at various service time: (a) mass loss ratio; (b) diameter reduction ratio; (c) strength reduction ratio.

5. CONCLUSION

Coastal bridges are essential for the transportation in offshore areas. They are highly threatened by multiple hazards accompanied with the degraded performance due to corrosion effects, leading to the necessity to safeguard them in their life-cycle periods. In this study, the chloride-induced corrosion around the coastal bridge pier was investigated with emphasis on their time-varying property within the design lifespan. The primary efforts and contribution of this study can be concluded as follows,

(1) A lifetime corrosion model was proposed to estimate the corrosion state at arbitrary service time within the lifespan.
(2) A case study was conducted to inspect the time-dependent corrosion for a prototype bridge, with the historical ocean salinity data obtained for the corrosion analysis.
(3) The corrosion probability takes 72% throughout the bridge lifespan, whereas it was reduced to 3% within the first 10 years. The median time of corrosion initiation takes 23 years, showing good resistance of the inspected bridge to corrosion effects.
(4) The fitting analysis shows good applicability to both the initial corrosion time and the consequent mass loss ratio, and the life-time corrosion model also has good effectiveness by regressing the time-dependent parameters.
(5) The probability density of corrosion at different service periods matches in certain ranges, while the cumulative probability increases significantly as the examined time prolongs.

ACKNOWLEDGMENTS

Financial supports from the National Key Research and Development Program of China (2023YFB2604400), the National Natural Science Foundation of China (Grant No. 52478507), the Natural Science Foundation of Heilongjiang Province (Grant No. LH2023E057) are greatly appreciated by the authors.

REFERENCES

[1] Akiyama Mitsuyoshi, Dan M. Frangopol, Hiroki Ishibashi: **Toward life-cycle reliability-, risk-and resilience-based design and assessment of bridges and bridge networks under independent and interacting hazards: emphasis on earthquake, tsunami and corrosion**. *Structure and Infrastructure Engineering*, Vol. 16, No. 1, 26-50, 2020.

[2] Chen Shilun, Colin Duffield, Saeed Miramini, Babar Nasim Khan Raja, Lihai Zhang: **Life-cycle modelling of concrete cracking and reinforcement corrosion in concrete bridges: A case study**. *Engineering Structures*, Vol. 237, 112143, 2021.

[3] El Maaddawy Tamer, Khaled Soudki: **A model for prediction of time from corrosion initiation to corrosion cracking**. *Cement and concrete composites*, Vol. 29, No. 3, 168-175, 2007.

[4] Tuutti Kyösti: **Corrosion of steel in concrete**. 1982.

[5] Kassir Mumtaz K., Michel Ghosn: **Chloride-induced corrosion of reinforced concrete bridge decks**. *Cement and Concrete Research*, Vol. 32, No.1, 139-143, 2002.

[6] Lin, G., Y. H. Liu, and Z. H. Xiang: **A mathematical model for prediction of time from corrosion initiation to corrosion cracking in RC structures**. *Materials and Corrosion*, Vol. 61, No. 11, 920-928, 2010.

[7] Khan Muhammad Umar, Shamsad Ahmad, Husain Jubran Al-Gahtani: **Chloride ‐ Induced Corrosion of Steel in Concrete: An Overview on Chloride Diffusion and Prediction of Corrosion Initiation Time**. *International journal of corrosion*, No. 1, 5819202, 2017.

[8] Lin Hongwei, Yuxi Zhao, Peng Feng, Hailong Ye, Josko Ozbolt, Cheng Jiang, Jia-Qi Yang: **State-of-the-art review on the bond properties of corroded reinforcing steel bar.** Construction and Building Materials 213, 216-233, 2019.

[9] Fang Congqi, Karin Lundgren, Liuguo Chen, Chaoying Zhu: **Corrosion influence on bond in reinforced concrete**. *Cement and concrete research*, Vol. 34, No. 11, 2159-2167, 2004.

[10] Enright Michael P., Dan M. Frangopol: **Probabilistic analysis of resistance degradation of reinforced concrete bridge beams under corrosion**. *Engineering structures*, Vol. 20, No. 11, 960-971, 1998.

[11] Ghosh Jayadipta, Jamie E. Padgett: **Aging considerations in the development of time-dependent seismic fragility curves**. *Journal of Structural Engineering*, Vol. 136, No. 12, 1497-1511, 2010.

[12] Dizaj Ebrahim Afsar, Rahmat Madandoust, Mohammad M. Kashani: **Probabilistic seismic vulnerability analysis of corroded reinforced concrete frames including spatial variability of pitting corrosion**. *Soil Dynamics and Earthquake Engineering*, Vol. 114, 97-112, 2018.

[13] Liu Jun, Zhilu Jiang, Yulong Zhao, Hao Zhou, Xiaodong Wang, Haijun Zhou, Feng Xing, Shanglin Li, Jihua Zhu, Wei Liu: **Chloride distribution and steel corrosion in a concrete bridge after long-term exposure to natural marine environment**. *Materials*, Vol. 13, No. 17, 3900, 2020.

[14] Tian Ye, Guoyi Zhang, Hailong Ye, Qiang Zeng, Zhidong Zhang, Zushi Tian, Xianyu Jin, Nanguo Jin, Zhonggou Chen, Jiaxi Wang: **Corrosion of steel rebar in concrete induced by chloride ions under natural environments.** *Construction and Building Materials*, Vol. 369, 130504, 2023.

[15] Pinto Francisco, Rodrigo Astroza, Ramiro Bazáez, Francisco Hernández Nibaldo Navarro: **Probabilistic seismic assessment of multispan RC highway bridges considering soil-structure interaction and chloride-induced corrosion**. *Engineering Structures*, Vol. 301, 117257, 2024.

[16] Domaneschi Marco, Antonino De Gaetano, Joan R. Casas, Gian Paolo Cimellaro: **Deteriorated seismic capacity assessment of reinforced concrete bridge piers in corrosive environment**. *Structural Concrete*, Vol. 21, No. 5, 1823-1838, 2020.

[17] Angst Ueli M.: **Predicting the time to corrosion initiation in reinforced concrete structures exposed to chlorides**. *Cement and Concrete Research,* Vol. 115, 559-567, 2019.

[18] Andisheh Kaveh, Allan Scott, Alessandro Palermo: **Effects of corrosion on stress–Strain behavior of confined concrete**. *Journal of Structural Engineering,* Vol. 147, No. 7, 04021087, 2021.

[19] Wei Guo, Honggen Qin, Wei Sun, Yiwen Yang: **Effects of Admixture and Water to Binder Ratio on Chloride Ion Permeability of Concrete** (in Chinese).

[20] Geiker Mette R., Max AN Hendriks, Bernhard Elsener: **Durability-based design: the European perspective**. *Sustainable and Resilient Infrastructure*, Vol. 8, No. 2, 169-184, 2023.